Photometric Flicker Metrics: Analysis and Perspectives

Pascal Dupuis, *Senior Member* ‡, Leoš Kukačka†, Michal Vik†, Aleš Richter†, Georges Zissis, *Senior Member* *.
*Université de Toulouse, LAPLACE, UMR 5213 (CNRS, INPT, UPS), 118 rte de Narbonne, 31062 Toulouse, France
† Technical University of Liberec, FMIIS, Studentska 1402/2 46117 Liberec, Czechia
‡Kawantech S.A.S, 6 Rue Françoise d'Eaubonne, 31200 TOULOUSE, FRANCE

***Abstract*—This paper complement another presentation, and focus mainly on the mathematical framework behind flicker metrics. The purpose is to review the algorithms extracting the features of the light level temporal fluctuations, and establish some of their properties. As the signals from the physical world will invariably be contaminated by noise, the robustness of the metrics to approach the "true" value will be assessed. By doing so, alternatives will be studied.**

***Index Terms*—Energy Saving Lamp (ESL); Compact Fluorescent Lamp (CFL); Light Emitting Diode (LED); Photometric Flicker; Flicker Percent (FP); Flicker Index (FI); Voltage Variation; Voltage Quality**

I. Introduction

Incandescent lamps powered by AC voltage exhibit flicker. The explanation is that the thermal time constant of the light emitting metal wire is in the timescale of milliseconds, while one half-period equals 10 milliseconds on a 50 Hz network. Instantaneous power fluctuations are translated into temperature oscillations, leading to temporal fluctuations of the emitted flux. The first flicker metrics approached those oscillation as some amplitude modulation of a signal around an average value. Such approaches were further reused on the next technologies, fluorescent and discharge lamps. The advent of Solid State Lighting Lighting introduced new challenges. The most important in the authors opinion is that the on/off modulation may be used as a way to regulate the average current, leading to asymmetric square waves.

This approach based upon amplitude modulation only describes phenomenon whose typical base frequency is at twice the distribution network frequency. In the framework of Power Quality as analysed by many authors [1], [2], [3], [4], [5], it became obvious that low frequency disturbances of the voltage *envelope* are translated into hum, or visible, slowly varying changes of the light level. Another concern is that the lamp driver, whose primary function is to absorb energy at the network frequency and adapt it to the lamp characteristics[6]., may use regulation loops which are improperly designed, leading to oscillations without external driving frequency.

Drapela [7] developped a light flickermeter following the IEC61000-3-3:2013 standard. In this approach, the temporal light waveform is splitted using a series of low-pass and band-pass filters, leading to a number of indexes. IEEE [8] defined a safe operating area based upon Percent Flicker, also known as Michelson contrast.

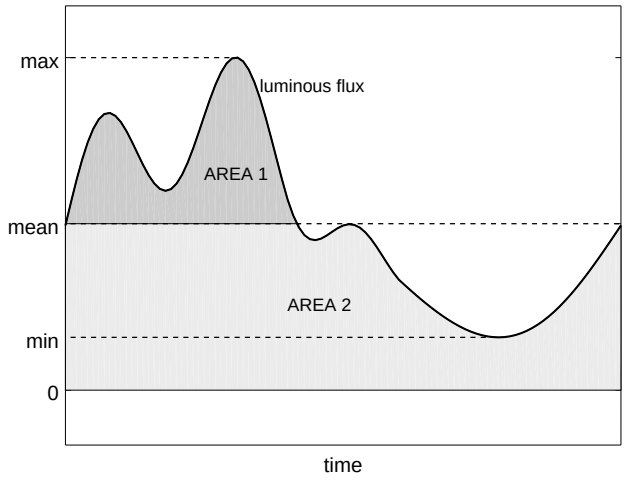

Fig. 1: Definition of flicker metrics according to IEEE Standard 1789-2015 [8].

Yet those metrics are supposed to reflect how humans would describe the temporal variations of the light flux. This means a number of elements are cascaded: a photometric sensor, an acquisition system performing the signal analog to digital conversion, and then some algorithm associate a value to the temporal data whose aim is to predict the perceptibility of the phenomenon. More accurately, the output should be a probability measure that usual observers will detect, find it acceptable, or complain, or be affected by those temporal fluctuations.

As explained, the research team performed an in-depth analysis of the sensitivity of two flicker metrics using the GUM approach. In this part, the emphasis will be put mostly on the mathematics behind the characterisation metrics, and analyse in a wide sense their meaning and their sensitivity to various noise sources.

II. Theoretical background

A. Definitions

IEC flicker definition requires to observe the temporal values over a window not smaller than two seconds, sampled at least at 20 kHz. Two metrics are defined from such data

stream. The Percentual Flicker is defined as the Michelson contrast of the luminous flux waveform:

$$FP = \frac{\max_{t\in(0;T)}(\Phi(t)) - \min_{t\in(0;T)}(\Phi(t))}{\max_{t\in(0;T)}(\Phi(t)) + \min_{t\in(0;T)}(\Phi(t))} \cdot 100, \quad (1)$$

where $\Phi(t)$ is the waveform and T is the length of the evaluation interval, being an integer multiple of the flicker period. This way, FP does not account neither for frequency nor for waveform shape.

The Flicker Index is defined as:

$$FI = \frac{\Lambda_1}{\Lambda_2}, \quad (2)$$

where

$$\Lambda_1 = \int_\Gamma (\Phi(t) - \bar{\Phi})\,\mathrm{d}t,\ \Gamma = \{t \in (0;T) : \Phi(t) > \bar{\Phi}\}, \quad (3)$$

$$\Lambda_2 = \int_0^T \Phi(t)\,\mathrm{d}t, \quad (4)$$

and T is an integer multiple of a period of fundamental frequency of the analysed flux waveform. Graphical interpretation of these definitions is in Fig. 1.

To probe further, let's describe the luminous flux as an amplitude-modulated signal:

$$y(t) = M + A[1 + \frac{s(t)}{A}]\sin(\omega t + \phi) \quad (5)$$

where

- $y(t)$ is the time dependant measured value;
- M is the mean value in the absence of modulating signal;
- A is the amplitude of the pulsating component;
- $s(t)$ is a zero-mean perturbation of the base level with upper level $smax$ and lower level $smin$;
- ω and ϕ are the pulsation and phase of the "carrier", which in most cases is at twice the network frequency.

In the absence of noise, FP can be expressed as

$$FP = \frac{\frac{smax-smin}{A}}{2 * [M + A[1 + \frac{smax+smin}{A}]]} \quad (6)$$

In the particular case where $smax$ is equal to $-smin$, this can further be simplified as

$$FP = \frac{\frac{smax}{A}}{[M + A]} \quad (7)$$

From which a few properties can be inferred:

1) the numerator reflects the modulation depth, *i.e.* the ratio between the modulating component and the base amplitude;
2) the denominator expresses the amplitude of the base signal;
3) the metric is insensitive to the shape of the perturbing signal.

Moreover, if the modulation depth reaches beyond some point, the minimum will tend towards zero, and by definition the FP value will saturate at $100\,\%$. In the case of on-off modulation, this metric will not provide any information on the duty cycle.

In the presence of noise, this approach can be considered as a worst-case scenario. The observation window will contain many maxima of the original signal, and the one with the greatest positive perturbation will be chosen. The same is true for the minimum, leading to the conclusion that such estimator is biased as the minus sign in the numerator will amplify the effect of the noise.

The analysis of the FI is straightforward thanks to the linearity of the integral operator. The M term of eq. 5 contributes to the total area, but not to the term Λ_1. Under the hypothesis that the observation window encompasses an integer number of periods and that $s(t)$ is zero mean, the pulsating term will not contribute to the global integral, while all parts where $s(t)$ is greater than zero will contribute to Λ_1. The numerator will thus reflect the interactions between the modulating and modulated frequencies, including the shape of the perturbing waveform, while the denominator is controlled by the average value only. In the case of on-off signal with on-value A over τ seconds, off-value 0 and period T, the indicator is given by

$$FI = 1 - \frac{\tau}{T} \quad (8)$$

If the modulation is symmetric, this value equals 1; if τ increases towards T, off-periods are called "silences" and the index tends towards zero, while when decreasing towards 0, the on-periods are called "pulses" and the metrics reaches one.

In the presence of noise, the whole integral will mitigate the noise effect. But there will be some residual noise on the average; this noise being coupled with Λ_1 through two paths. The first one is that an error on the surface, equal to the average value multiplied by the width on the Λ_1 interval, will be added. Secondly, the width itself will change as a function of the signal slope close to the average value. Furthermore, the illustration of fig.1 shows a signal with a few clean transitions around the average value. Once again, in the presence of noise, there may be many transitions on short time scales. The definition does not provide hints or explain how to mitigate this effect.

B. Other aspects

So far it was hypothesised that the observed signal was a mix of well defined frequencies. But real lamps may be more complex than that. As explained, most of Solid State Lighting ballasts use switching regulators for efficiency reasons, with their own internal function generator. Over the year, the research team at Laplace lab observed that any SSL driver start by a AC to DC converter, followed by an energy storage element as the conduction is discontinuous, which powers both the lighting element and its controller. If the energy storage element is insufficient, the LED may exhibit recurrent patterns over one switching cycle. As explained earlier, the design of the regulation loop may also present insufficient gain at low frequencies, leading to self-sustained oscillations. And lastly, even if those effects are not present, the regulation loop may also be inadequate at rejecting the voltage oscillations after

the AC to DC converter. This occurs mostly with single-stage drivers associated to small size lamps.

C. Physiological considerations

The translations of light stimuli into an image of the scene as perceived by the brain is quite a complex process. Let's just point out a few elements:

1) the eye pupil adapts itself to the average scene luminance;
2) the cells acting as light sensors have some remanence: after being hit by a photon, it takes a few milliseconds to be ready to produce a new signal;
3) the eye themselves actively scan the scene; one single view in the brain results usually from the merging of around 20 partial images.

In the authors opinion, a flicker metric should take into account three parameters: the average light level, the frequency, and the wave patterns. Short light pulses will briefly produce an excitation of the light detectors; while short light silences will produce long excitation followed by a pause.

D. Improving actual metrics

At this point, it has been established that FI is can effectively reject noise provided an integer number of periods can be observed, which may be difficult to ensure in the presence of switching regulators.

The sensitivity of FP to noise could be reduced according to two ways:

1) focusing on the signal envelope. But this relies on Hilbert's transform, with the effect of squaring the noise and introducing bias;
2) using synchronous detection which will bring the envelope back at DC. But this is only applicable is the carrier can be reconstructed.

III. Probabilistic signal description

As pointed out many times, the two studied metrics are based on assumptions such as the ability to represent the basic signal as periodic and sampling an integer number of periods. Those assumptions are not universal, in particular with SSL lighting. We would like to present an approach of signal characterisation using a field of mathematics called computational topology.

Let start by a simple example. Close to the sea there is a rock with is covered at high tide and emerging at low tide. When the sea retreats, a first peak appear and gradually transform into an island. Then other peaks appears, together with other islands separated by straight. At some point, the straight becomes free of water: two islands are merging. By convention, the earliest appearing island is said to absorb the other one, which is said to "die", *i.e.* stopping being an island. This process can be performed when water retreats, focusing on local maxima, or goes up, focusing on local minima. To each peak is associated a persistence level, defined as the height difference between birth and death levels. The highest peak has the greatest persistence, which corresponds to the signal peak-to-peak range. The temporal information is irrelevant. The signal is then represented in a 2D diagram where points are associated to the (birth, death) values.

IV. Extending FP using Fourier transform

As explained, the FP metric was designed in the perspective of characterizing amplitude-modulated signal. As already pointed out, as such it is insensitive to the perturbing signal shape. In the presence of on-off modulation with light extinction, this metric reaches a maximum of $100\,\%$, irrespective of the actual duty cycle.

We propose an approach based upon the Fourier transform in a similar fashion to the recently introduced Stroboscopic Visibility Measure metric. Let's define its objectives as:

- for consistency, the value for small-signal amplitude modulation where the envelope is a sine should be equal to the actual FP computation;
- the computation should mitigate the influence of wide-band white noise;
- in the case of small-signal AM where the envelope is rectangular, the result should be slightly influenced by the duty cycle
- For on-off modulation, the value should be small for "silences" and higher for pulses.

This can be accomplished as follows. Let $Y(n)$ represent the Discrete Fourier Transform of the temporal signal $x(n)$, $0 <= n < N$ where N is the number of samples. $Y(0)$ is equal to the DC value, or the signal average. The extended FP metric is simply defined as

$$FPE = \frac{\sqrt{\sum_{i=N1}^{N2} |Y(i)|^2}}{Y(0)} \tag{9}$$

where $N1$ and $N2$ are two suitably chosen values such that:

- frequencies below $N1$ are considered as irrelevant. Due to windowing effect, there will be some ripple around the peak at $Y(0)$. $N1$ should be just above this peak width.
- frequencies above $N2$ are considered as irrelevant for flicker computation. One such limit could be $3\,\mathrm{kHz}$ as defined in IEEE Std-1789 [8].

V. Results

A. Computational topology

To illustrate those methods, let start from a noised AM signal as illustrated on fig. 2 with 20000 samples. The observation window runs over 1000 milli-seconds of a base signal at $100\,\mathrm{Hz}$. the AC peak value is one tenth of the DC component amplitude, leading to a FP of $10\,\%$. The four peaks with the greatest extent are labelled by their number. Red circles are local minima; green circles are local maxima. The extrema are associated to their extent in fig. 3 by the red lines, while the green horizontal segments link the birth and death places.

The phase diagram of fig. 4 is built around one diagonal line. Peaks are represented by their (birth, death) values. There is a group of ten values in the lower right corner and another group in the upper left, indicating ten periods have been recorded.

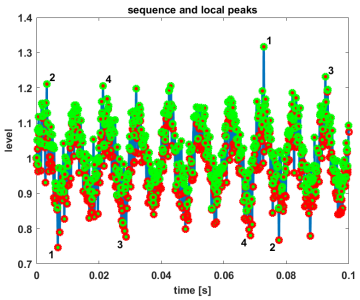

Fig. 2: Noised signal peaks

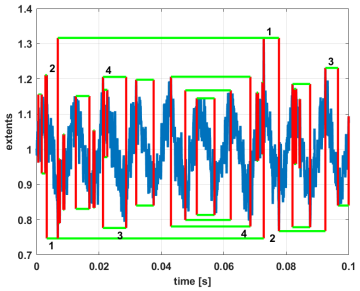

Fig. 3: Noised signal extents

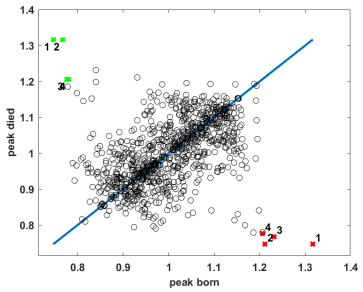

Fig. 4: Noised signal peaks

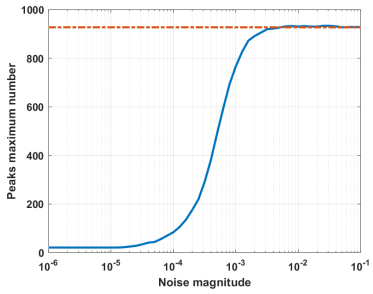

Fig. 5: Noised signal extents

This cloud of points corresponds to values occurring in the vicinity of the noise-free extrema. The points in close to the diagonal are characterised by a small extent and are thus mostly occurring due to noise. This diagram also permits to establish the distribution of the extrema.

Lastly, this process was repeated by changing the noise level on a logarithmic scale. When no noise is present, there are ten peaks; the noise signal by itself contains around 400 peaks. The number of peaks appears as an indicator of the signal to noise ratio as illustrated in Fig. 5.

B. Noise Sensitivity

Fig. 6 illustrates how the three approaches cope with noise. The abscissa contains the amplitude of the added noise to the previously described waveform. The straight method uses the global maximum and minimum. The "Perstopology" extracts $20\,\%$ of the peaks and compute their average value. The Fourier transform was explained at the end of the previous section. The noise-free FP level is $10\,\%$.

A number of observations can be performed:

- noise is not a concern for any of the three methods below 10^{-3};
- the computational topology alleviates a bit the issue up to 10^{-2}, but does not provide significant improvement over the upper decade;
- the Fourier transform approach is insensitive to noise up to 10^{-2}, and its growth rate is slower. At the highest noise level, were the time signal is barely recognizable, the FP is $50\,\%$

C. FP and on-off signals

THe results are displayed in Tab. I. The duty cycle values first cover one point per decade of pulse. Then there is a linear space between 0.1 and 0.9. The last values are logarithmic spaced silences. The original FP metric provide a constant value of $10\,\%$ for small-signal variations and $100\,\%$ for on-off modulation

TABLE I: Duty Cycle, small-signal, on-off signal

Duty	Small	ON-OFF
0.0001	0.85	1072
0.0010	0.88	1072
0.0100	2.4	1022
0.1000	9.0	414
0.2000	11.9	278
0.3000	13.3	212
0.4000	13.9	170
0.5000	13.9	139
0.6000	13.4	113
0.7000	12.3	91
0.8000	10.5	69
0.9000	7.7	46
0.9900	2.0	10
0.9990	0.86	1.37
0.9999	0.85	1.00

The analysis of the second column indicates that there exists now some relationship between the duty cycle and the extended indicator. The maximum is reached for duty cycles between 0.4 and 0.5. Both pulses and silences result in quite small values.

The third column brings something different:

- For short silences, the results are quite small
- The value grows rapidly as duty cycle decreases. The main reason is that the DC value collapses accordingly.

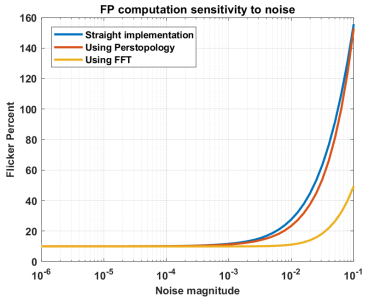

Fig. 6: Comparison of noise sensitivities

Let us remind that this DC value appears at the denominator of Equ. 9.

- for intermediate duty cycles values between .6 and .1, the extended FP goes above $100\,\%$.

VI. Discussion

The results obtained so far show that the extended metric based upon Fourier Transform can mimic the behaviour of the original one on small signal sine-modulated waveforms, yet decrease the sensitivity to noise with respect to the straight, extrema based approach.

In the case of rectangular modulation, the extended metric now reflects somewhat the value of the duty cycle. In the case of Visible Light Communication using modulation at "high" frequencies, such component would not contribute to the lamp flicker. But we have to accept that this new metric produces results greater than $100\,\%$ in the case of on-off switching, which is nowadays common with LEDs control scheme to implement dimming.

VII. Conclusions

The flicker perceptual indicator has been analysed from a mathematical point of view, with an emphasis on the robustness to noise. An extension aiming at tracking the shape of the temporal waveform has also been proposed. The original definition relies on the ability to capture an integer number of periods. As SSL sources may contain their own switching regulator, such approach is difficult to implement. In this paper, two alternatives approaches were presented.

One is based on peak detection using a topological approach. Such treatment mostly ignores the time and signal scales, relying solely on comparison operations between neighboring points. The 2D time-independent representation generate clouds of points from which properties such as probability densities and noise level can be evaluated. It has been shown that it permits to mitigate noise problems up to some extent.

The second uses the Fourier transform to evaluate the ratio between AC and DC components. It may be used as a robust alternative to extrema based computations for sine-modulated components. If we accept the idea of an indicator greater than $100\,\%$, it was shown that this new approach provides some insight over the duty cycle of on-off signal which is missing in the original definition.

The next step is to confront this extended indicator to the ability to detect and predict persons perception of flicker.

Acknowledgment

The authors would like to acknowledge support by the H2020-WIDESPREAD project no. 857061 "Networking for Research and Development of Human Interactive and Sensitive Robotics Taking Advantage of Additive Manufacturing".

References

[1] A. F. H. Nohra, H. Y. Kanaan, and K. Al-Haddad, "A study on the impact of a massive integration of compact fluorescent lamps on power quality in distribution power systems," in *2012 International Conference on Renewable Energies for Developing Countries (REDEC)*. IEEE, nov 2012, pp. 1–6. [Online]. Available: http://ieeexplore.ieee.org/lpdocs/epic03/wrapper.htm?arnumber=6416700

[2] R. Saxena and K. Nikum, "Comparative study of different residential illumination appliances based on power quality," in *2012 IEEE 5th India International Conference on Power Electronics (IICPE)*. IEEE, dec 2012, pp. 1–5. [Online]. Available: http://ieeexplore.ieee.org/lpdocs/epic03/wrapper.htm?arnumber=6450385

[3] M. H. J. Bollen, H. Hooshyar, S. K. Rönnberg, S. Ronnberg, H. Hooshyar, and M. H. J. Bollen, "Spread of high frequency current emission," in *22nd International Conference and Exhibition on Electricity Distribution (CIRED 2013)*. Institution of Engineering and Technology, 2013, pp. 0209–0209.

[4] S. K. Rönnberg, M. Wahlberg, and M. H. J. Bollen, "Laboratory and field measurements of the power factor and the harmonic emission from energy-efficient lamps," Tech. Rep. May, 2011.

[5] L. Monjo, J. J. Mesas, L. Sainz, and J. Pedra, "Study of voltage sag impact on LED lamp consumed currents," in *2016 International Symposium on Fundamentals of Electrical Engineering (ISFEE)*. IEEE, jun 2016, pp. 1–6. [Online]. Available: http://ieeexplore.ieee.org/document/7803234/

[6] C. Brañas, F. J. Azcondo, and J. M. Alonso, "Solid-State Lighting: A System Review," *IEEE Industrial Electronics Magazine*, vol. 7, no. 4, pp. 6–14, dec 2013. [Online]. Available: http://ieeexplore.ieee.org/document/6681992/

[7] J. Drapela, S. Jan, and J. Slezingr, "Design and utilization of a light flickermeter," in *2012 IEEE International Workshop on Applied Measurements for Power Systems (AMPS) Proceedings*. IEEE, sep 2012, pp. 1–6. [Online]. Available: http://ieeexplore.ieee.org/document/6344007/

[8] IEEE Std 1789, *IEEE Recommended Practices for Modulating Current in High-Brightness LEDs for Mitigating Health Risks to Viewers*. IEEE, 2015.